# Supporting information

## Revealing the excited-state emission pathways in indolizine-derived TADF molecules by photoluminescence and electroluminescence

*Emmanuel Santos Moraes[1], Elisa Barbosa de Brito[2], Jilian Nei de Freitas[2], Rene Alfonso Nome[1], Manoela Sacramento[3], Fabiano Severo Rodembusch*[3], Paulo Henrique Schneider*[3], Teresa Dib Zambon Atvars*[1].*

## Summary

## 1. Materials and Methods

### 1.1 Materials

All molecules were purchased from commercial sources and used without further purification. The Polystyrene (PS) (Mw 260,000), was obtained from Scientific Polymer Products, Poly(3,4-ethylenedioxythiophene) polystyrene sulfonate (PEDOT:PSS PVP AI 4083) were purchased from Clevios, dry Dichloromethane, Polymethylmethacrylate (PMMA) (Mw very high), 1,3-Bis(N-carbazolyl)benzene (mCP) 97%, 2,2',2''-(1,3,5-Benzinetriyl)-tris(1-phenyl-1-H-benzimidazole) (TPBi) 99%, Calcium and Aluminum were purchased from Sigma-Aldrich.

### 1.2 Methods

*Computational approach*: The structure with minimum energy was predicted to use a Global Optimizer Algorithm (GOAT) in conjunction with a GFN2-xTB semiempirical approach.[1] The global minimum structure was further optimized using density functional theory (DFT) with the PBE0-D3[2,3] functional and the Karlsruhe basis set Def2-TZVP[4] at a vacuum level.[5] Additionally, vertical transitions were analyzed using time-dependent DFT (TD-DFT) to predict the singlet and triplet energy. About the donor-bridge-acceptor (D-π-A) nature of these molecules, a potential energy surface (PES) was predicted for various dihedral angles between the D-π pair to find some conformer energy barriers. The same basis set was employed for the orbital assignments in the transitions, the energies of the triplet states, and the spin-orbit coupling (SOC). All calculations were performed using ORCA version 6.0,[6,7] and the results were visualized with Gabedit 2.5.2, [8] Avogadro 1.2, [9] and Multiwfn software.[10,11]

*Film deposition*: PMMA, PS, and mCP films: The solutions were prepared at concentrations of 100, 20, and 20 mg $mL^{-1}$ in dichloromethane for PMMA, PS, and mCP, respectively. The solutions were stirred for one day until complete dissolution occurred. Additionally, solutions of the molecules **Z**, **ZCz**, **ZPX**, and **ZPT** were prepared at a concentration of 1 mg $mL^{-1}$ in dichloromethane. Aliquots of 100 µL of the PMMA, PS, and mCP solutions were combined with 100 µL of the dye solution, resulting in a final weight concentration of 1, 5, and 5% in PMMA, PS, and mCP, respectively. For the deposition process, an aliquot of 100 µL of the mixture solution was spin-coated at 3000 rpm for 30 seconds onto clean glass substrates.

*Photophysics*:

Electronic absorption spectra were collected using a Carry 60 UV-Vis Agilent Technologies spectrophotometer equipped with a thin-film sample holder.

Steady-state fluorescence spectra were recorded with a Cary Eclipse Varian spectrofluorimeter, and the excitation was at different wavelengths as indicated in the study. The films were oriented in a back-face configuration. The photoluminescence quantum yield ($\Phi_{PL}$) was obtained in an integration sphere, and the sample was excited at 375 nm, in air at room temperature (RT), according to the absolute method using a Fluorolog-3 Horiba FL3-22iHR320 spectrofluorometer with dual excitation and dual emission monochromators. A 450 W (Ushio) ozone-free xenon lamp and a Hamamatsu R928P photomultiplier were used as light sources. The samples were excited at 375 (± 10) nm, and the corresponding emission profile was recorded from 365 to 710 nm.[12]

Time-resolved emission spectra (TRES): The decays were acquired using the time-correlated single-photon counting (TCSPC) technique on an Edinburgh Analytical Instruments FL 900 spectrofluorometer with an MCP-PMT (Hamamatsu R3809U-50), a pulsed diode operating at $\lambda_{exc}$ = 370.8 nm (EPL-375, FWHD 10 nm, and a pulse width of 77.0 ps). At 10 K, a Joplin cryostate CCG-450 refrigerated by helium and a LakeShore temperature controller.

Fluorescence Lifetime Imaging Microscopy (FLIM): The images were acquired via TCSPC in time-tagged time-resolved (TTTR) measurement mode using a MicroTime 200 Fluorescence Lifetime Microscope from PicoQuant, equipped with an LDH-D-C-405 laser head (70 ps pulse width) and operated with SymPhoTime software. Additionally, for the FLIM measurements, the PDL 828 Sepia Laser Driver was configured with an 80 MHz base oscillator, burst length (pulse count), and burst repetition rate set for microsecond delayed fluorescence lifetime measurements.

*Diode fabrication and characterization*: OLEDs were fabricated on a glass substrate with a patterned ITO (7 Ω/square) from Kintec Company. The ITO was cleaned with Hellmanex® 2% (30 min), hot deionized water, acetone, and 2-propanol, via ultrasonic bath, followed by washing with hot deionized water and treating with UV-ozone cleaner (10 min). PEDOT:PSS was deposited by static spin-coating at 5000 rpm for 30 s, followed by thermal annealing at 120 °C for 15 min. The active layers were based on **Z**, **ZCz**, **ZPX**, and **ZPT** in a host(mCP):guest system with 5% of each active material. The solution was processed in dry dichloromethane at a final concentration of 10 $mg.mL^{-1}$ and spin-coated at 3000 rpm for 30 s. TPBi was deposited by thermal evaporation (40 nm) at a ratio of 0.1-0.5 $Å.s^{-1}$ under a pressure of ~$10^{-6}$ mbar, and cathode calcium (10 nm) and aluminum (100 nm) were evaporated at 0.1 and 2.0 $Å.s^{-1,}$ respectively. The final device structure was ITO|PEDOT:PSS|mCP:Active(5%)|TPBi|Ca|Al. After deposition, the diodes were encapsulated using a UV-light-curing epoxy resin. The area of the pixel is 0.09 $cm^2$.

The electrical properties were analyzed by current vs. voltage (I×V) measurements using a 2400 Keithley Source Meter. The EL spectra were acquired using a USB2000+ Ocean Optics diode array spectrometer. The luminance data and CIE 1931 chromaticity coordinates were measured using a Konica Minolta LS-100 luminancimeter, coupled with a close-up lens No. 110 (ø=40.5 mm, 10–20 cm). All data were collected simultaneously using a homemade LabVIEW interface. OLED external quantum efficiency (EQE) calculations were also done in a homemade software, assuming a Lambertian emission profile, photopic correction of the EL, and perpendicular device measurement.[13–15]

## 2. Theoretical calculation

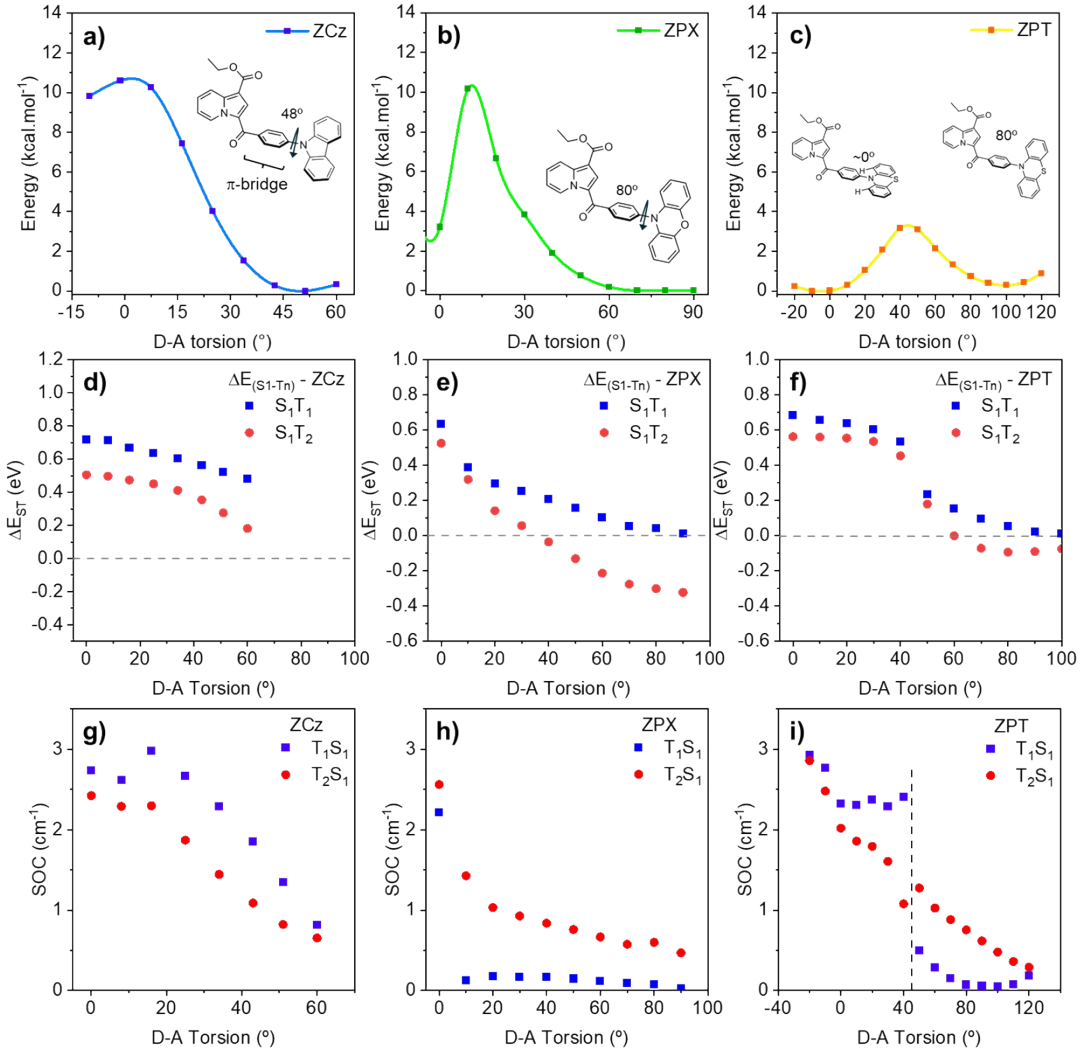


**Figure S1.** The potential energy surface (PES) of the donor group rotation with respect to the acceptor group. Configurational energy (a-c), singlet-triplet energy gap ($\Delta E_{ST}$) of $S_1T_1$ and $S_1T_2$ (d-f), and spin-orbit coupling (SOC) (g-i), for **ZCz**, **ZPX**, and **ZPT**, respectively.

## 3. Photophysics

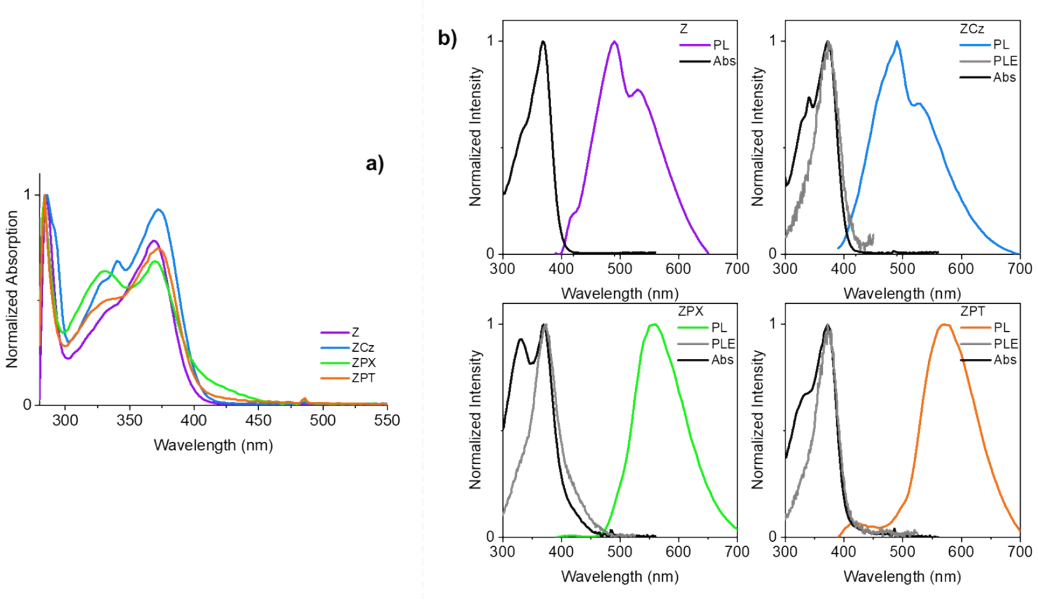


**Figure S2.** Room temperature absorption a), PL and PLE b) spectra in toluene at 1X10$^{-5}$ M, in air of the **Z**, **ZCz**, **ZPX**, and **ZPT**.

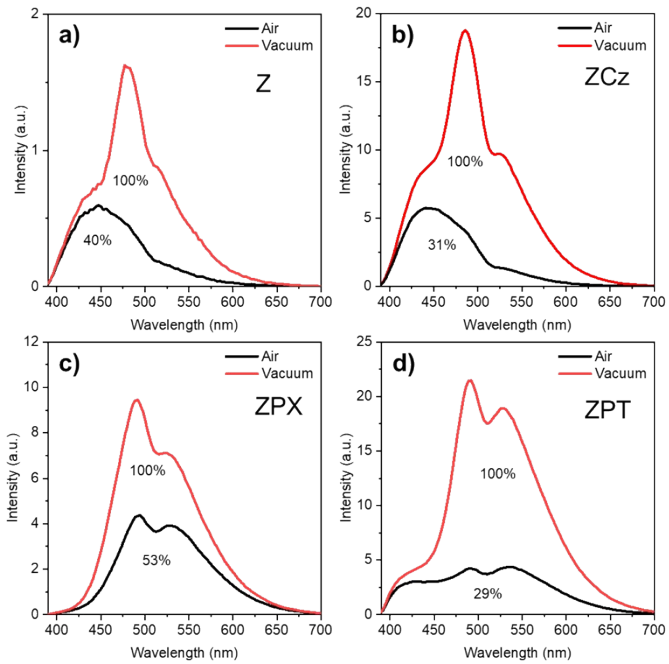


**Figure S3.** Room temperature PL spectra for in air and degassed samples of **Z**/PMMA a), **ZCz**/PMMA b), **ZPX**/PMMA c), and **ZPT**/PMMA d).

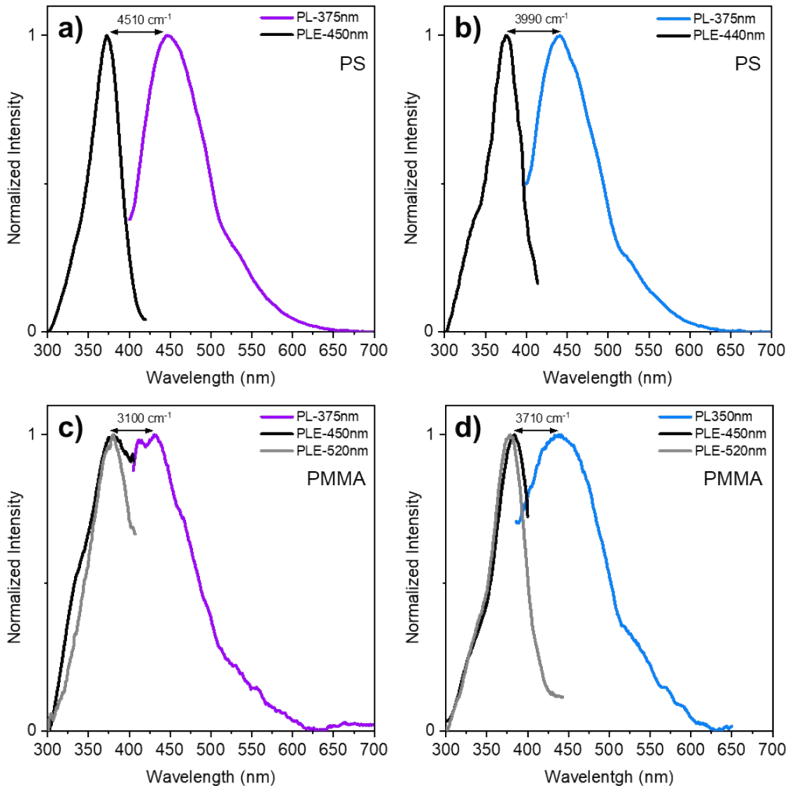


**Figure S4.** PL and PLE of (a) **Z**/PS, (b) **ZCz**/PS, (c) **Z**/PMMA, and (d) **ZCz**/PMMA recorded at RT, in the air condition. The arrow indicates the difference in energy between PL and PLE.

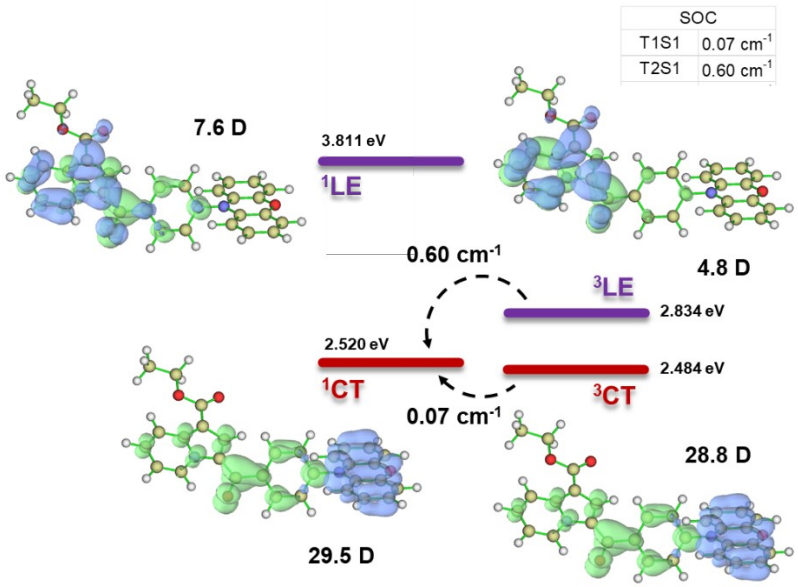


**Figure S5.** Natural transition orbitals (NTOs) of **ZPX**. The Hole (blue) and electron (green) distributions, the SOC between $^3$CT→$^1$CT and $^3$LE→$^1$CT, and the variation of the dipole moment ($\mu_{ES}$ - $\mu_{GS}$) in the excited states.

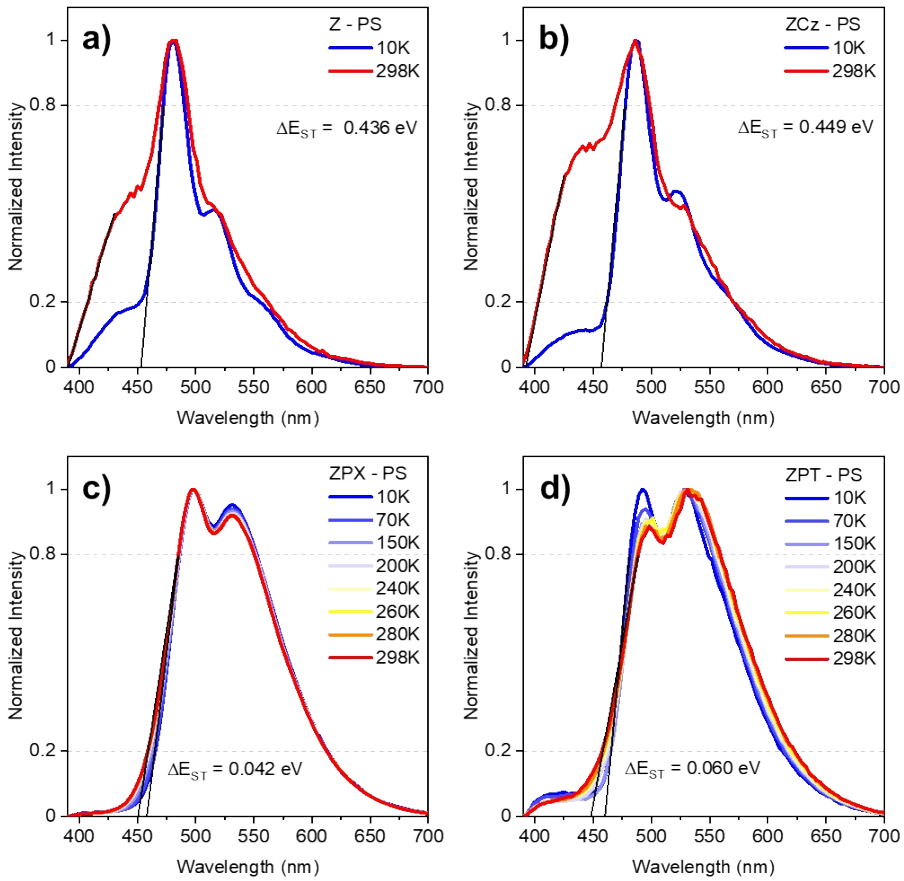


**Figure S6.** PL of molecules **Z** (a), **ZCz** (b), **ZPX** (c), and **ZPT** (d) at various temperatures in PS degassed samples.

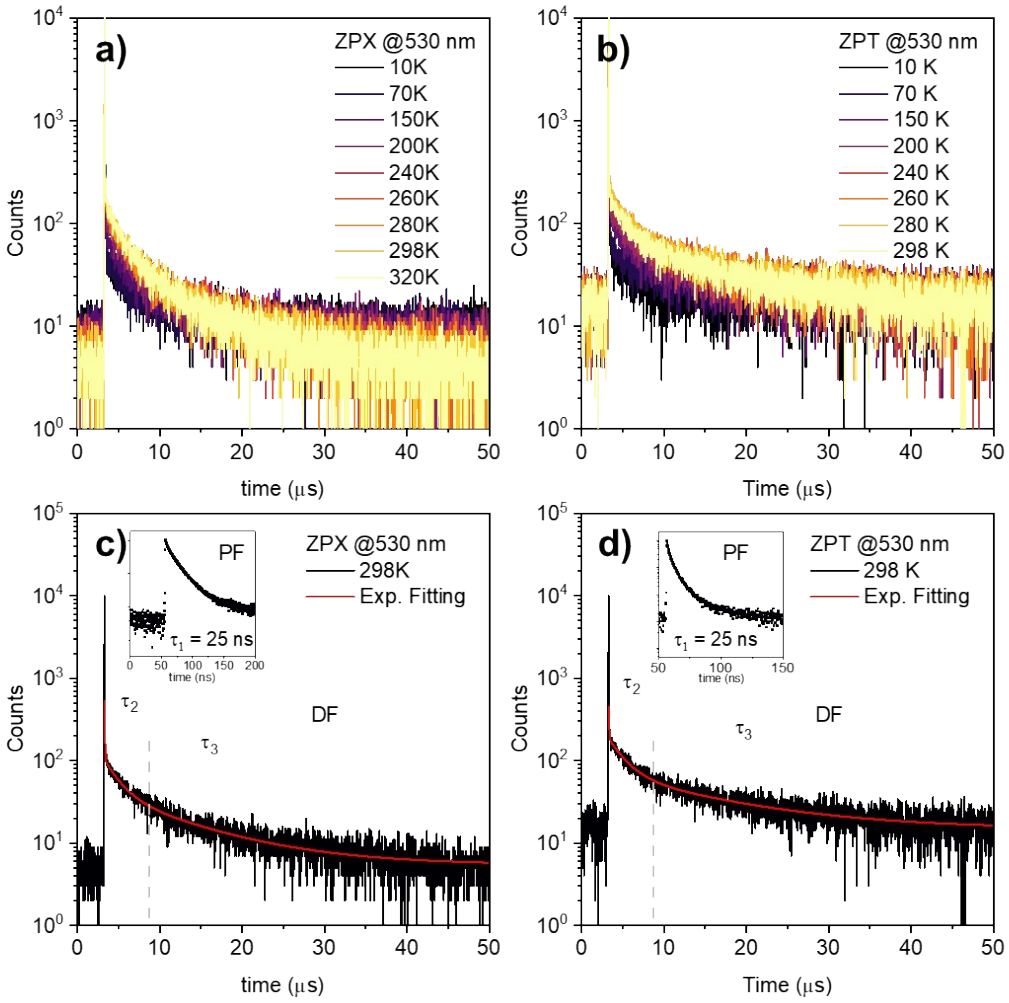


**Figure S7.** Emission decays of **ZPX**/PS (a) and **ZPT**/PS (b) degassed samples collected at 530 nm at various temperatures on the scale of 50 μs. Wavelength excitation at $\lambda_{exc}$ = 375 nm. A fitted decay with tri-exponential function at RT.

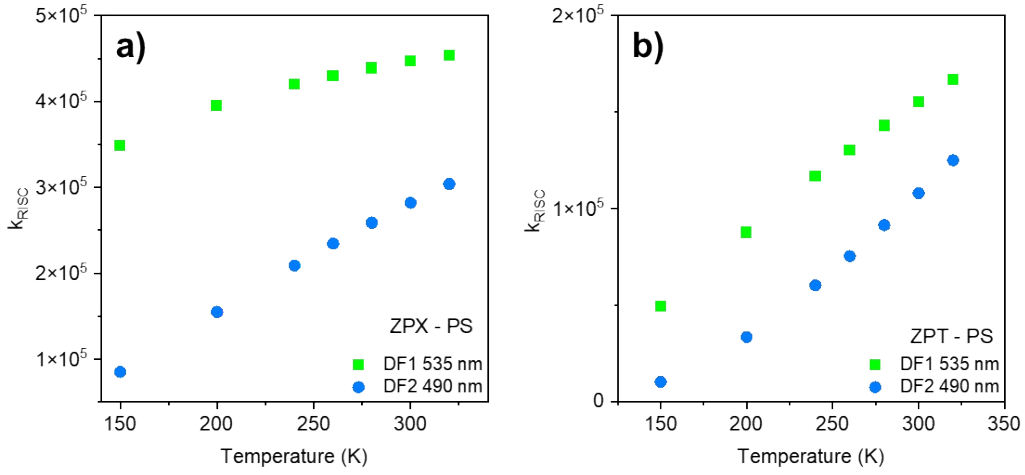


**Figure S8.** The $k_{RISC}$ versus temperature at 490 nm and 535 nm of **ZPX** (a) and **ZPT** (b).

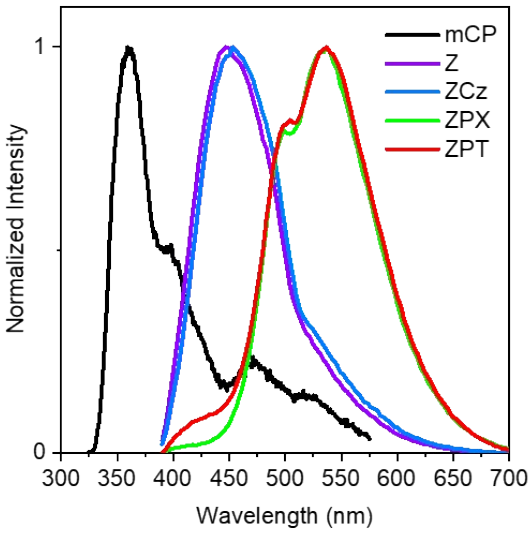


**Figure S9.** PL spectra of mCP ($\lambda_{exc}$ 300 nm), **Z**/mCP, **ZCz**/mCP, **ZPX**/mCP, and **ZPT**/mCP degassed samples ($\lambda_{exc}$ = 375 nm) at 298 K.

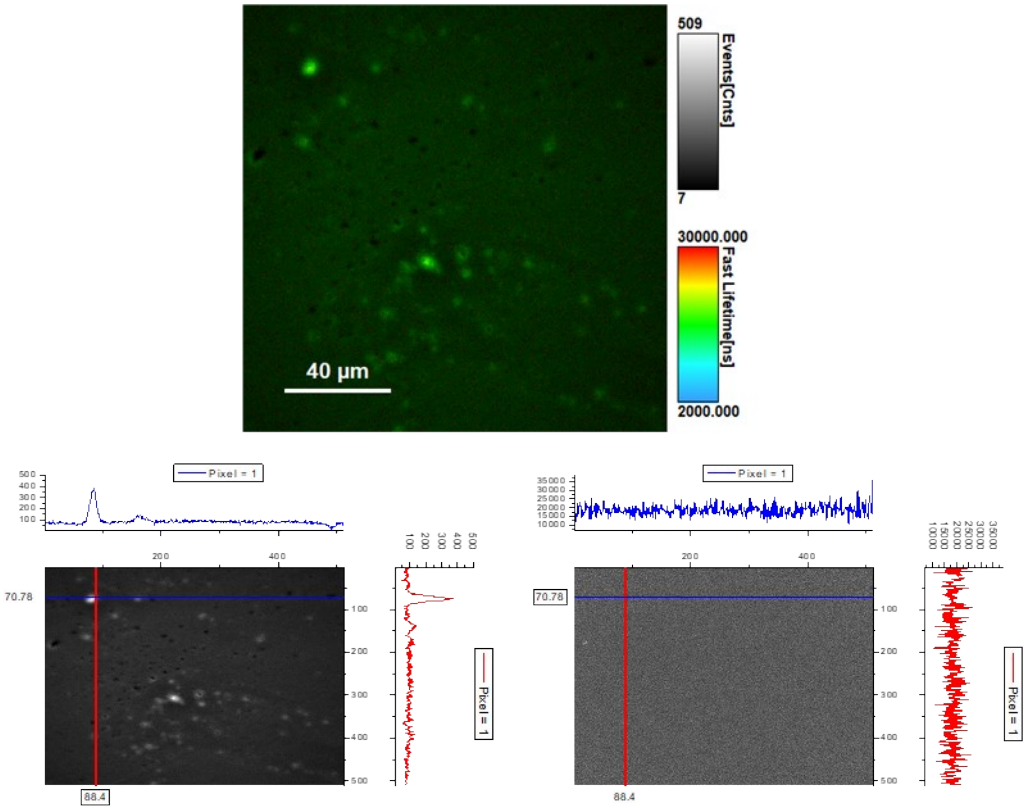


**Figure S10.** [DFLIM ZPT/mCP] image (top) and line profile analysis of intensities (bottom, left) and lifetimes (bottom, right).

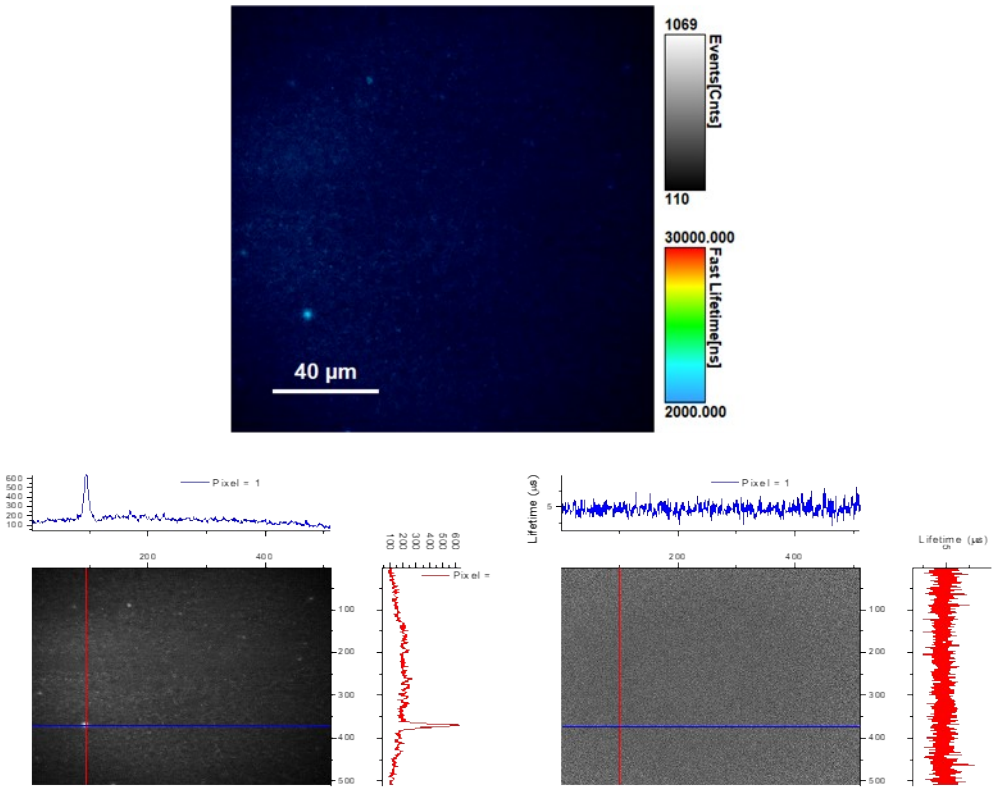


**Figure S11.** [DFLIM **ZPX**/mCP] image (top) and line profile analysis of intensities (bottom, left) and lifetimes (bottom, right).

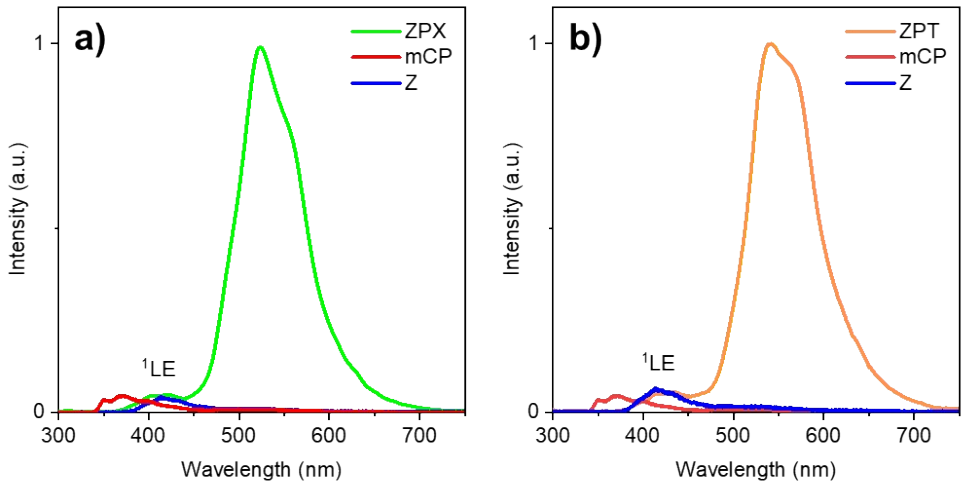


**Figure S12.** Comparison between the EL of mCP, **Z** (model for $^1$LE emission), and **ZPX** (a) and **ZPT** (b).

| | $V_{on}$ | $L_{max}$ | $CE_{max}$ | $PE_{max}$ | $EQE_{max}$ | $EQE_{calc}$ [a] | $\lambda_{max}$ | FWHM | CIE 1931 | |
|---|---|---|---|---|---|---|---|---|---|---|
| | V | cd $m^{-1}$ | cd $A^{-1}$ | lm $W^{-1}$ | % | % | nm | nm | x | y |
| Z | 8.5 | 15 | 0.42 | 0.16 | 0.3 | 0.4 | 422 | 60 | 0.209 | 0.170 |
| ZCz | 7.0 | 50 | 0.59 | 0.16 | 0.4 | 0.3 | 425 | 65 | 0.183 | 0.197 |

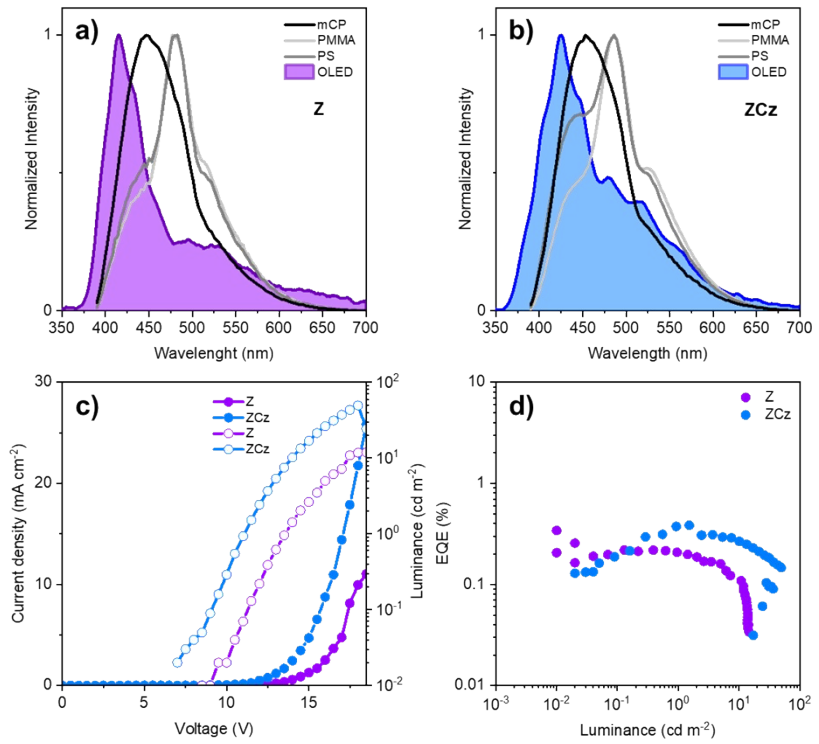


**Figure S13.** Table with data for the performance of OLEDs; emission spectra comparing EL with the PL of **Z** and **ZCz** in PMMA, PS, and mCP hosts a, b); and electrical curves IxV (c) and luminance x EQE (d) for the OLEDs.

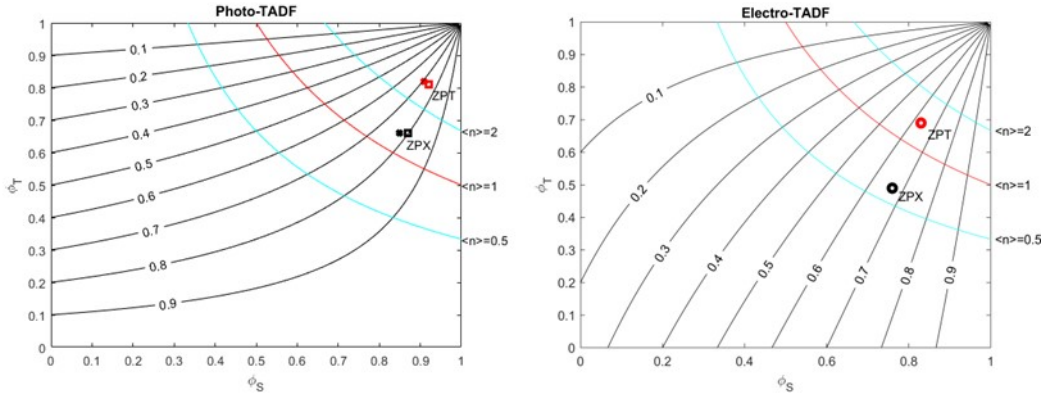


**Figure S14.** [STI] Singlet-triplet interconversion diagrams for photoluminescence TADF (left) and electroluminescence TADF (right).

## 4. Synthesis and Characterization

### 4.1 General information

Unless otherwise stated, all glassware was dried before use, and all reactions were performed under an atmosphere of argon. All solvents were distilled from appropriate

drying agents prior to use. All reagents were used as received from commercial suppliers unless otherwise stated. Reaction progress was monitored by thin-layer chromatography (TLC) performed on aluminum plates coated with silica gel F254 with 0.2 mm thickness. Chromatograms were visualized by fluorescence quenching with UV light at 254 nm, iodine, and by staining using vanillin solution. Flash column chromatography was performed using silica (230- 400 mesh, Merck and co.) or automated flash chromatography (Biotage® Selekt) using silica gel 60 (230 - 400 Mesh). High resolution mass spectra (HMRS) were recorded on a Micromass Q-Tof spectrometer, using electrospray ionization (ESI). Melting points were determined on a Buchi Melting Point M−545. All $^{1}H$ NMR and $^{13}C$ NMR spectra were recorded using a 400 MHz or 300 MHz spectrometer at 298K (frequency for $^{1}H$). Chemical shifts were given in parts per million (ppm, δ), referenced to TMS, defined at δ = 0.0 ppm ($^{1}H$ NMR) and to the solvent peak of $CDCl_3$, defined at δ = 77.0 ($^{13}C$ NMR). Coupling constants are quoted in Hz (J). $^{1}H$ NMR splitting patterns were designated as singlet (s), broad singlet (brs), doublet (d), triplet (t), quartet (q), doublet of doublets (dd), triplet of doublets (td), doublet of doublets of doublets (ddd). Splitting patterns that could not be interpreted or easily visualized were designated as multiplet (m).

## 5. General Procedure

### 5.1 Ethyl 3-(4-bromobenzoyl)indolizine-1-carboxylate (Z)

In a rounded-bottom flask, 1.0 mmol of the 2,4′-dibromoacetophenone was dissolved in 1.5 mL of acetonitrile. Subsequently, 1.0 mmol of pyridine was added to the solution. The resulting mixture was subjected to sonication for 5 min with the ultrasound set at an amplitude of 50 %. Next, 1.2 mmol of cesium carbonate and 0.5 mmol of the ethyl propiolate were added to the reaction mixture. The entire mixture was sonicated again at an amplitude of 50 % for 5 min. The crude mixture was then diluted with water and subjected to extraction using ethyl acetate (3 × 25 mL). After extraction, the mixture was dried and subjected to purification by chromatography using a column with a mobile phase of 10–20 % ethyl acetate in hexane.

### 5.2 General procedure compounds ZCz, ZPX, and ZPT

In a two-necked reaction tube (5 mL) equipped with a two-way stopcock and a magnetic stir bar, were added ethyl 3-(4-bromobenzoyl)indolizine-1-carboxylate (Z) (0.186g), fused tricyclic heteroaromatics (carbazole, phenoxazine and phenothiazine) (1.05 equiv.), sodium tert-butoxide (1.5 mol%), $Pd_2(dba)_3$ (0.5 mol%) and three vacuum-argon cycles were performed. After, anhydrous toluene (1.5 mL) was added under a stream of argon gas at 120 °C, and the resulting mixture was stirred for 24 h. Water (5 mL) was added to the reaction mixture, and the organic layer was extracted with $CH_2Cl_2$ (20 mL × 3). The combined organic extracts were dried over $Mg_2SO_4$, and the solvent was evaporated under vacuo to give the crude product, which was purified by flash column chromatography.

**Ethyl 3-(4-bromobenzoyl)indolizine-1-carboxylate (Z)**

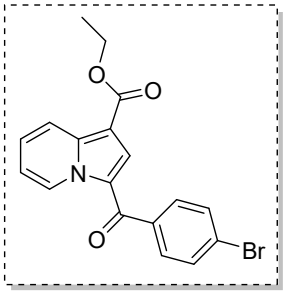

Yield: 76% (282 mg) as a beige solid. $^{1}$H NMR (400 MHz, $CDCl_3$ δ 9.93 (dt, *J* = 7.0, 1.1 Hz, 1H), 8.40 (dt, *J* = 9.0, 1.3 Hz, 1H), 7.77 (s, 1H), 7.73 – 7.60 (m, 4H), 7.47 (ddd, *J* = 9.0, 7.0, 1.1 Hz, 1H), 7.10 (td, *J* = 7.0, 1.5 Hz, 1H), 4.38 (q, *J* = 7.1 Hz, 2H), 1.40 (t, *J* = 7.1 Hz, 3H). $^{13}$C NMR (100 MHz, $CDCl_3$) δ 184.3, 164.1, 142.1, 140.2, 138.8, 131.8, 130.6, 129.3, 129.0, 128.1, 126.4, 122.3, 119.7, 115.6, 106.7, 60.3, 14.7.

**Ethyl 3-(4-(9*H*-carbazol-9-yl)benzoyl)indolizine-1-carboxylate (ZCz)**

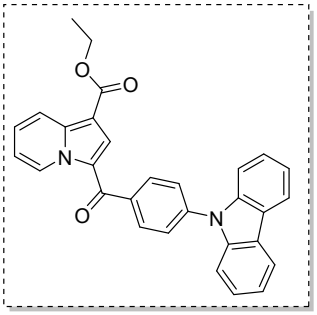

Yield: 30% (137 mg) as a yellow solid; mp: 214 – 216 °C $^{1}$H NMR (400 MHz, $CDCl_3$) δ 10.03 (dt, *J* = 7.0, 1.2 Hz, 1H), 8.43 (dt, *J* = 9.0, 1.2 Hz, 1H), 8.20 – 8.13 (m, 2H), 8.12 – 8.05 (m, 2H), 7.98 (s, 1H), 7.76 (d, *J* = 8.4 Hz, 2H), 7.59 – 7.42 (m, 5H), 7.37 – 7.29 (m, 2H), 7.15 (td, *J* = 7.0, 1.4 Hz, 1H), 4.42 (q, *J* = 7.1 Hz, 2H), 1.44 (t, *J* = 7.1 Hz, 3H). $^{13}$C NMR (100 MHz, $CDCl_3$) δ 184.44, 164.27, 146.29, 142.85, 139.97, 136.38, 131.37, 129.33, 128.76, 127.92, 127.82, 127.24, 126.75, 124.44, 123.86, 122.60, 121.14, 119.68, 115.42, 106.43, 60.32, 14.72. HRMS (ESI+): exact mass calculated for [M+H]+ ($C_{30}H_{23}N_2O_3$) requires m/z 459.1703, found: m/z 459.1704.

**Ethyl 3-(4-(10H-phenoxazin-10-yl)benzoyl)indolizine-1-carboxylate (ZPX)**

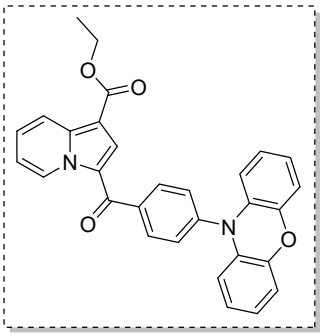

Yield: 24% (114 mg) as a yellow solid; mp: 222 – 225 °C. $^{1}$H NMR (400 MHz, $CDCl_3$) δ 10.02 (d, *J* = 7.0 Hz, 1H), 8.43 (d, *J* = 8.9 Hz, 1H), 8.05 (d, *J* = 8.0 Hz, 2H), 7.92 (s, 1H), 7.52 (d, *J* = 8.0 Hz, 3H), 7.18 – 7.06 (m, 1H), 6.85 – 6.47 (m, 6H), 6.04 (d, *J* = 7.4 Hz, 2H), 4.42 (q, *J* = 7.1 Hz, 2H), 1.44 (t, *J* = 7.1 Hz, 3H). $^{13}$C NMR (100 MHz, $CDCl_3$) δ 184.3, 164.0, 143.9, 142.1, 140.0, 139.8, 133.8, 131.7, 130.9, 129.3, 129.1, 128.0, 123.3, 122.3, 121.7, 119.6, 115.6, 115.6, 113.4, 106.7, 60.3, 14.6. HRMS (ESI+): exact mass calculated for [M+H]+ ($C_{30}H_{23}N_2O_4$) requires m/z 475.1652, found: m/z 475.1649.

**Ethyl 3-(4-(10*H*-phenothiazin-10-yl)benzoyl)indolizine-1-carboxylate (ZPT)**

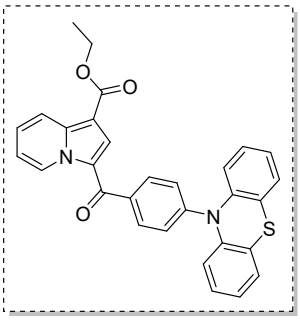

Yield: 43% (210 mg) as a yellow solid; m.p: 177 – 180 °C $^{1}$H NMR (400 MHz, $CDCl_3$) δ 9.96 (d, *J* = 7.1 Hz, 1H), 8.40 (d, *J* = 8.9 Hz, 1H), 7.95 – 7.83 (m, 3H), 7.52 – 7.41 (m, 1H), 7.37 (d, *J* = 8.6 Hz, 2H), 7.28 – 7.21 (m, 2H), 7.16 – 7.05 (m, 3H), 7.02 (t, *J* = 8.1 Hz, 2H), 6.82 (d, *J* = 9.4 Hz, 2H), 4.40 (q, *J* = 7.1 Hz, 2H), 1.42 (t, *J* = 7.1 Hz, 3H).$^{13}$C NMR (100 MHz, $CDCl_3$) δ 184.4, 164.3, 146.3, 143.0, 140.0, 136.4, 131.4, 129.3, 128.8, 127.9, 127.8, 127.2, 126.7, 124.4, 123.9, 122.6, 121.1, 119.7,

115.4, 106.4, 60.3, 14.7. HRMS (ESI+): exact mass calculated for [M+H]+ ($C_{30}H_{22}N_2O_3S$) requires m/z 490.1351, found: m/z 490.1338.

## 6. NMR Spectra

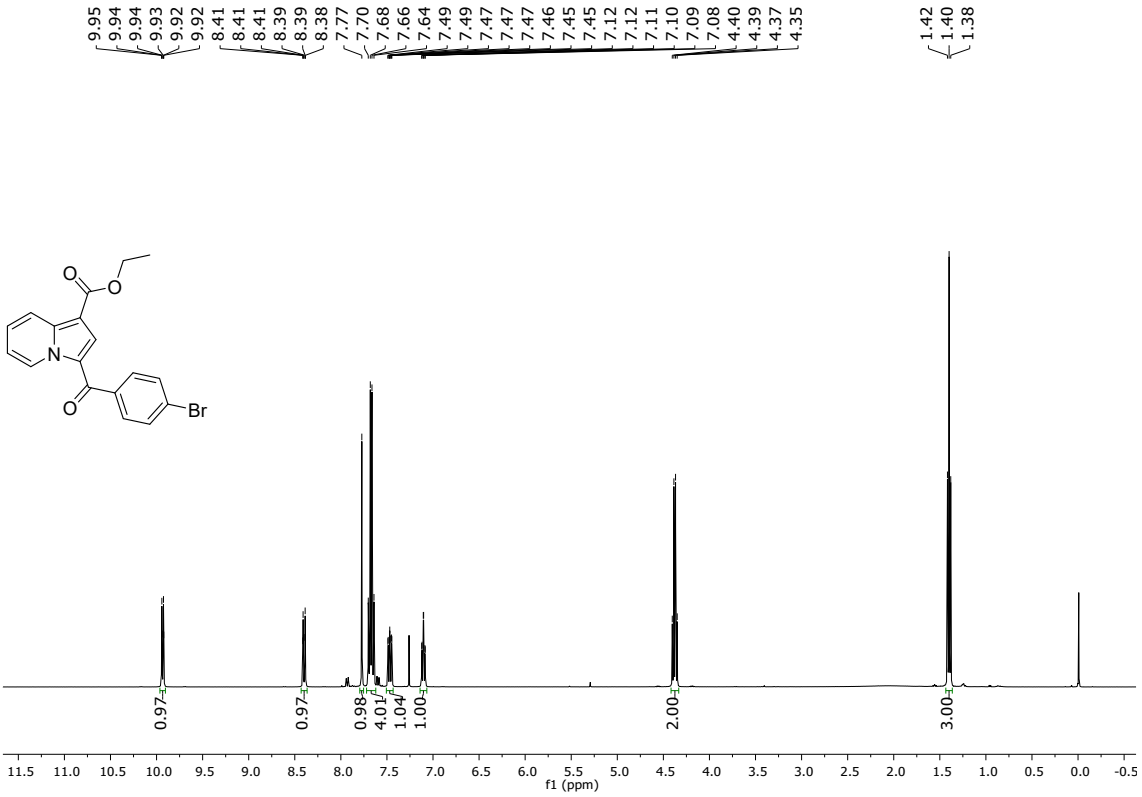


**Figure S15.** $^1$H NMR spectrum for compound **Z** ($CDCl_3$, 400 MHz).

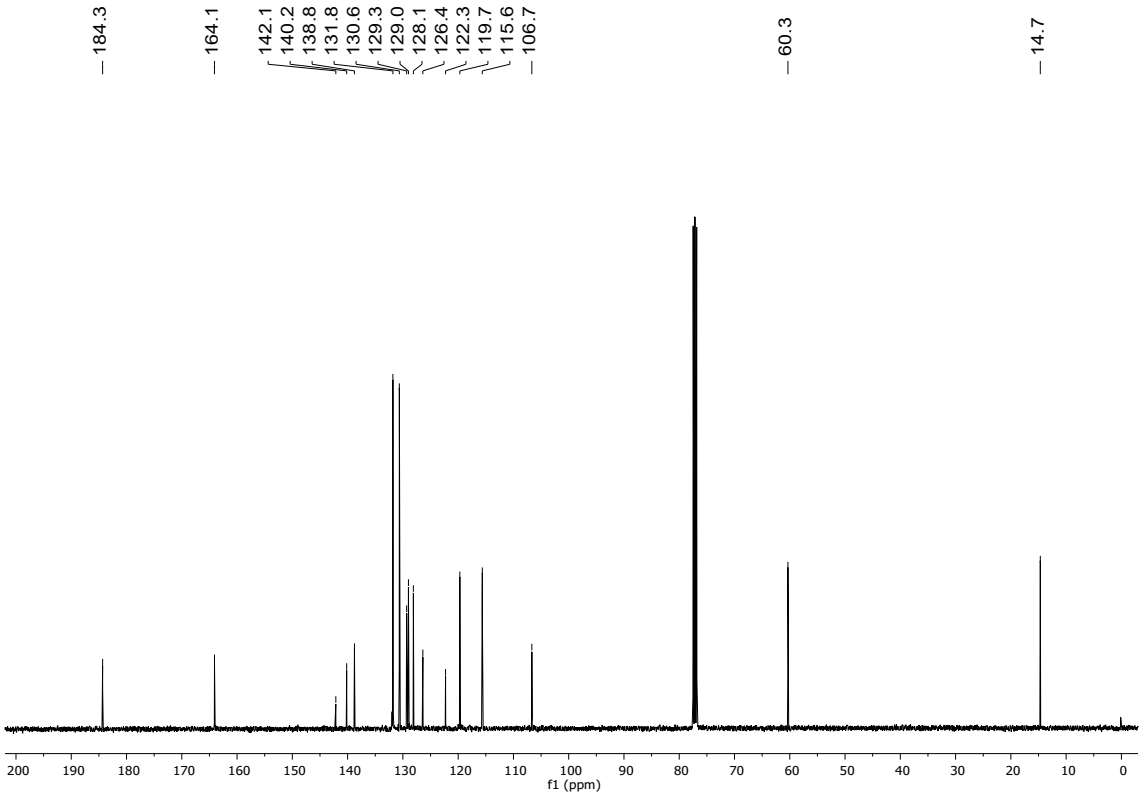


**Figure S16.** $^{13}C$ NMR spectrum for compound **Z** ($CDCl_3$, 100 MHz).

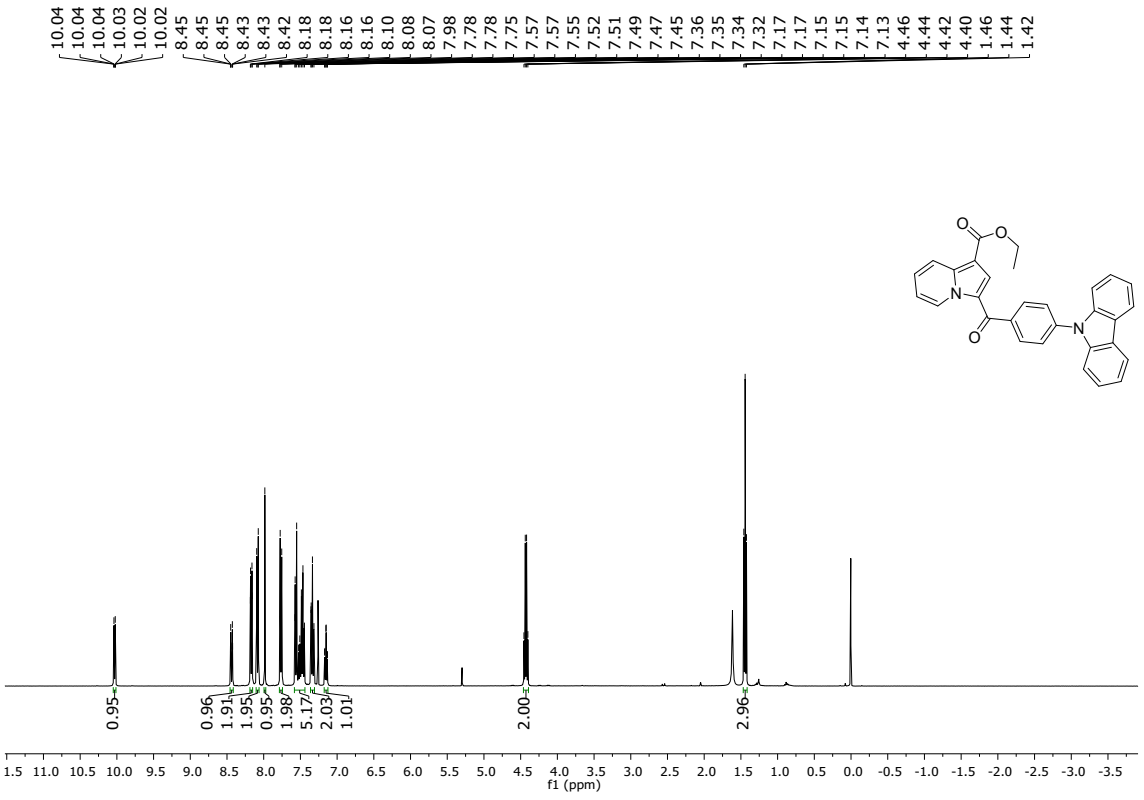


**Figure S17.** $^{1}H$ NMR spectrum for compound **ZCz** ($CDCl_3$, 400 MHz).

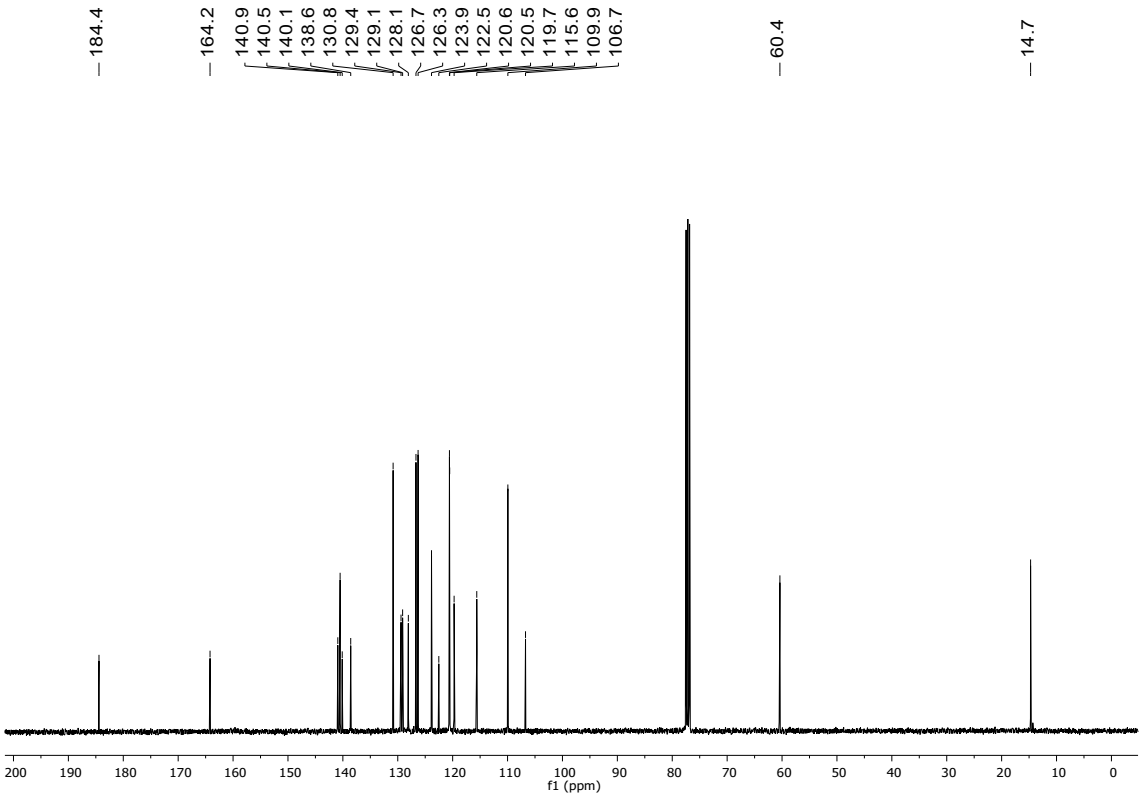


**Figure S18.** $^{13}C$ NMR spectrum for compound **ZCz** ($CDCl_3$, 100 MHz).

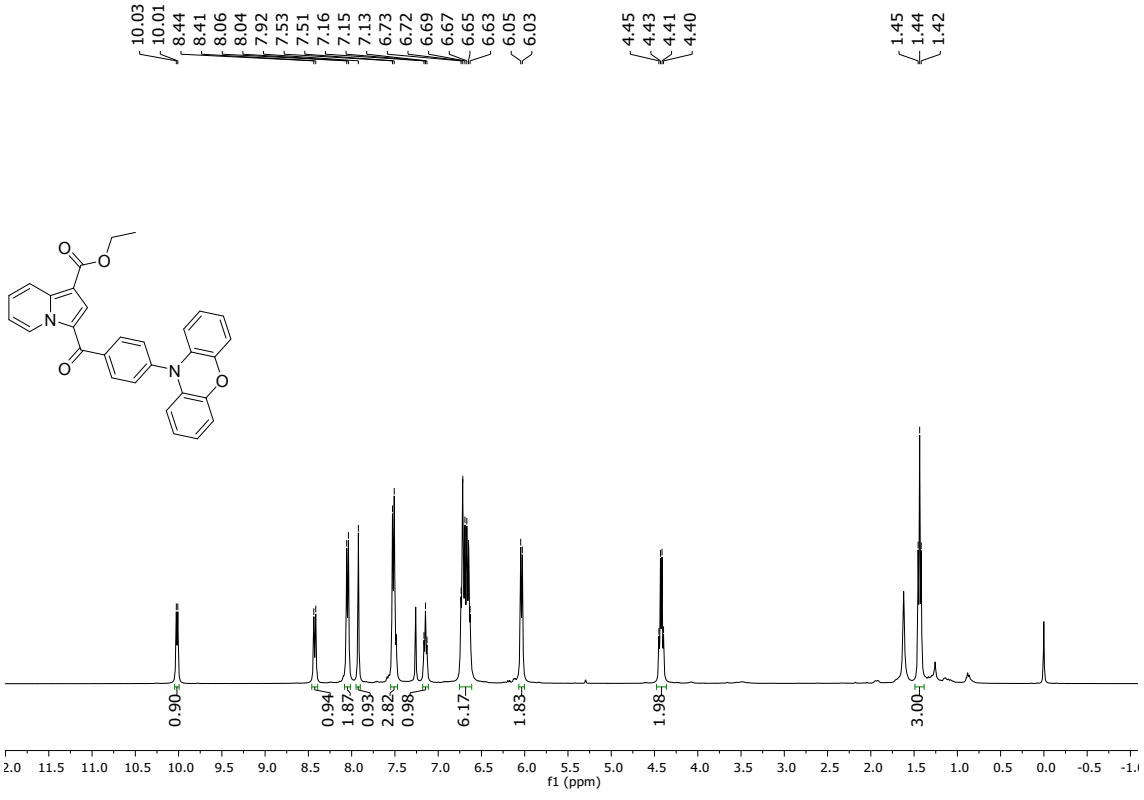


**Figure S19.** 1H NMR spectrum for compound **ZPX** (CDCl3, 400 MHz).

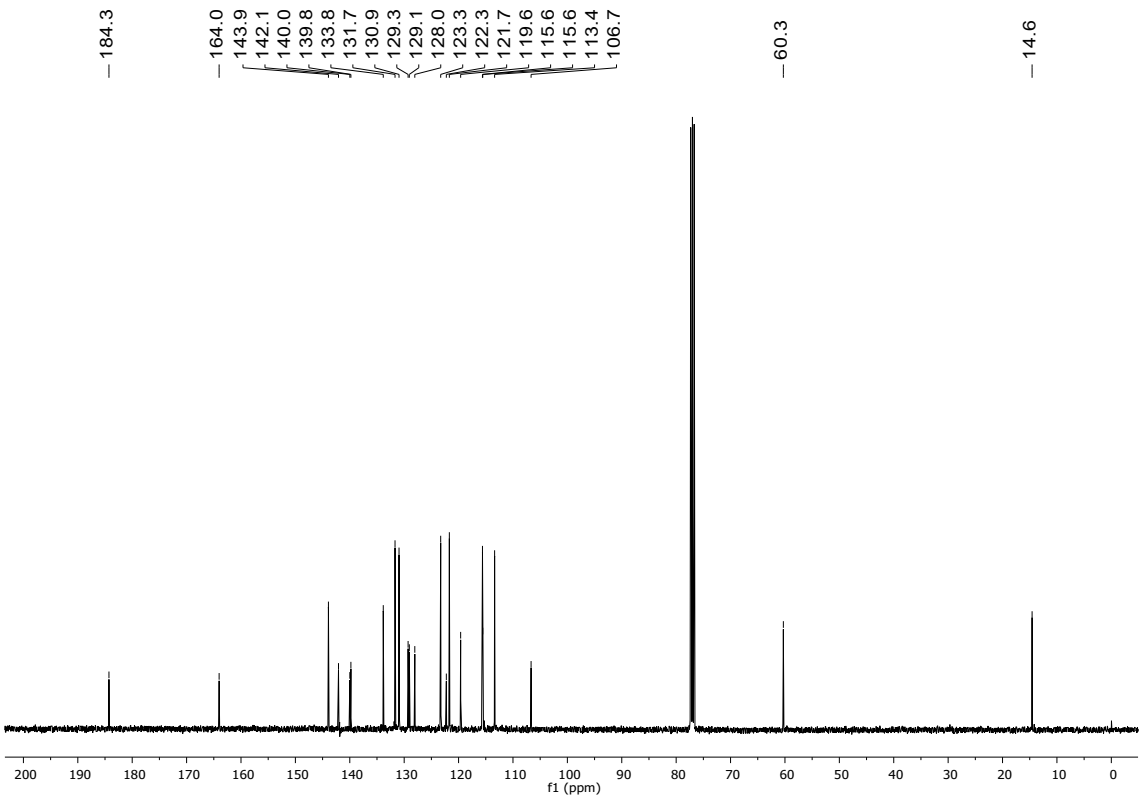


**Figure S20**. $^{13}C$ NMR spectrum for compound **ZPX** ($CDCl_3$, 100 MHz).

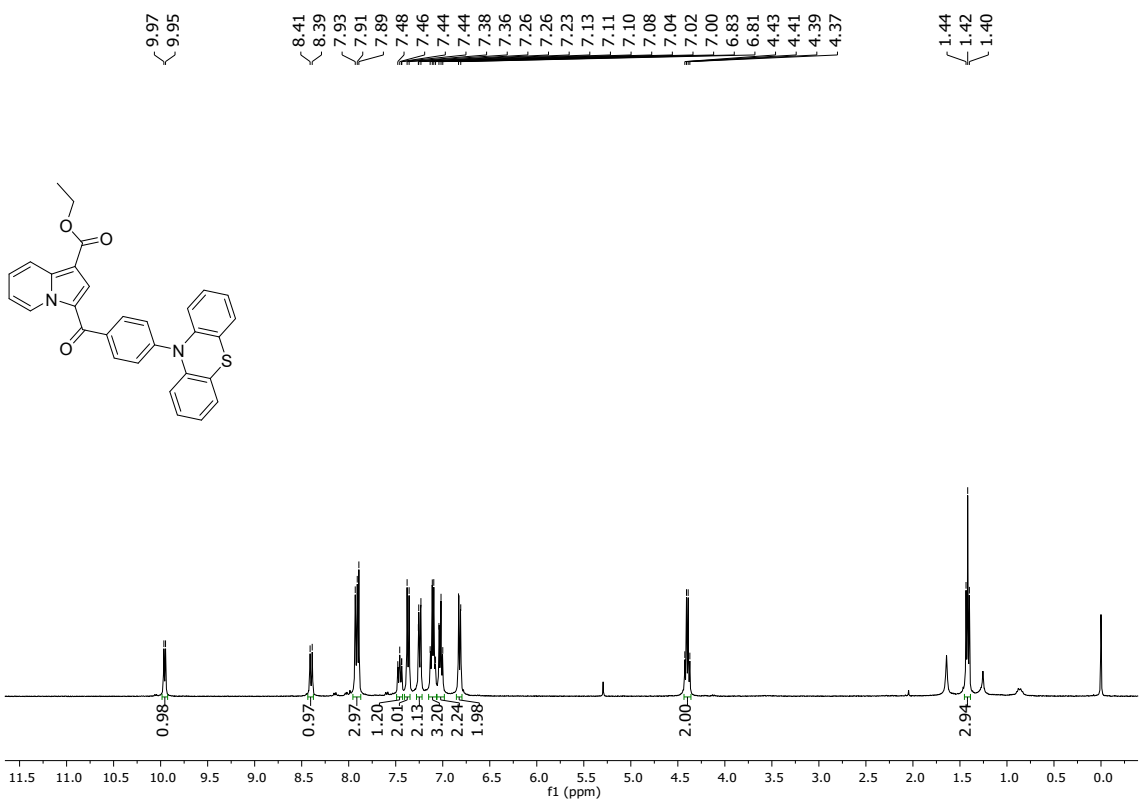


**Figure S21**. $^{1}$H NMR spectrum for compound **ZPT** ($CDCl_3$, 400 MHz).

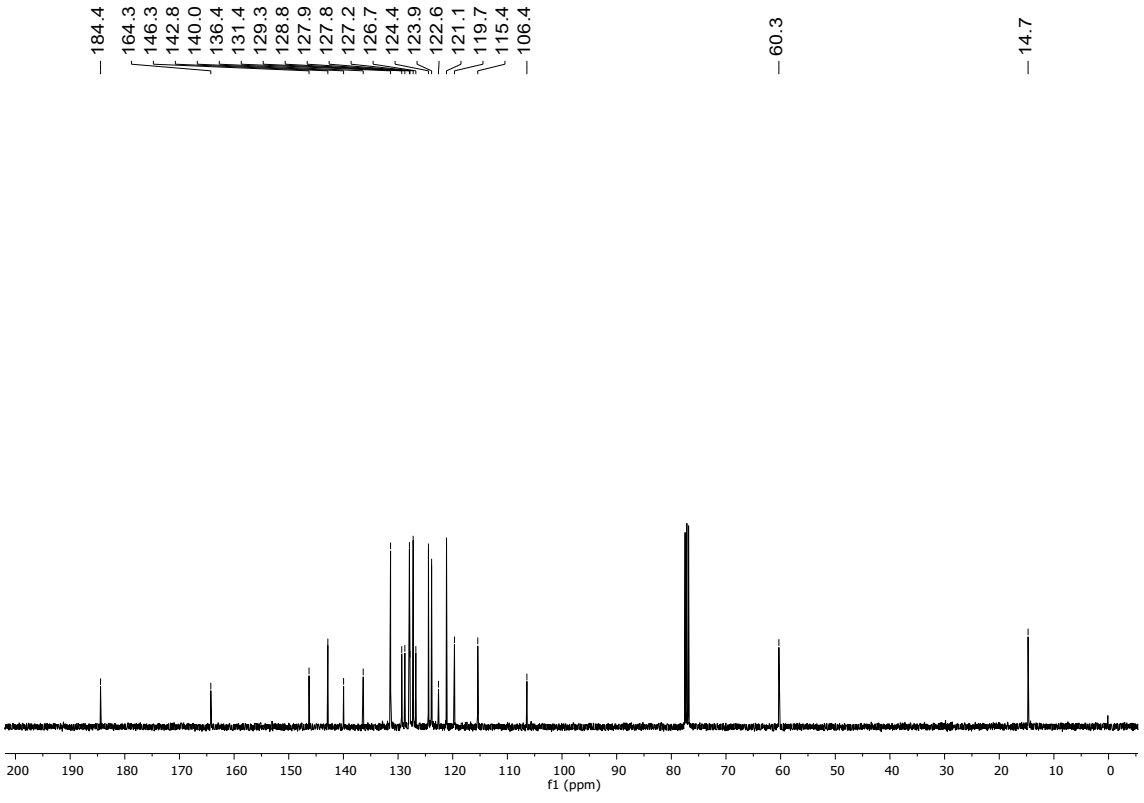


**Figure S22**. $^{13}$C NMR spectrum for compound **ZPT** ($CDCl_3$, 100 MHz).

**References**


1 C. Bannwarth, E. Caldeweyher, S. Ehlert, A. Hansen, P. Pracht, J. Seibert, S. Spicher and S. Grimme, *WIREs Computational Molecular Science*, DOI:10.1002/wcms.1493.

2 J. P. Perdew, K. Burke and M. Ernzerhof, *Phys. Rev. Lett.*, 1996, **77**, 3865–3868.

3 S. Grimme, S. Ehrlich and L. Goerigk, *J. Comput. Chem.*, 2011, **32**, 1456–1465.

4 F. Weigend and R. Ahlrichs, *Physical Chemistry Chemical Physics*, 2005, **7**, 3297–3305.

5 F. Neese, F. Wennmohs, A. Hansen and U. Becker, *Chem. Phys.*, 2009, **356**, 98–109.

6 F. Neese, *John Wiley and Sons Inc*, 2022, preprint, DOI: 10.1002/wcms.1606.

7 F. Neese, *Wiley Interdiscip. Rev. Comput. Mol. Sci.*, 2012, **2**, 73–78.

8 A. Allouche, *J. Comput. Chem.*, 2012, **32**, 174–182.

9 M. D. Hanwell, D. E. Curtis, D. C. Lonie, T. Vandermeersch, E. Zurek and G. R. Hutchison, *J. Cheminform.*, 2012, **4**, 17.

10 T. Lu, *J. Chem. Phys.*, DOI:10.1063/5.0216272.

11 T. Lu and F. Chen, *J. Comput. Chem.*, 2012, **33**, 580–592.

12 J. C. De Mello, H. F. Wittmann and R. H. Friend, *Advanced Materials*, 1997, **9**, 230–232.

13 M. Anaya, B. P. Rand, R. J. Holmes, D. Credgington, H. J. Bolink, R. H. Friend, J. Wang, N. C. Greenham and S. D. Stranks, *Nature Research*, 2019, preprint, DOI: 10.1038/s41566-019-0543-y.

14 International Commission on Illumination (CIE), CIE spectral luminous efficiency for photopic vision.

15 W. Jin, Y. Deng, B. Guo, Y. Lian, B. Zhao, D. Di, X. Sun, K. Wang, S. Chen, Y. Yang, W. Cao, S. Chen, W. Ji, X. Yang, Y. Gao, S. Wang, H. Shen, J. Zhao, L. Qian, F. Li and Y. Jin, *npj Flexible Electronics*, DOI:10.1038/s41528-022-00169-5.